Bifurcation in the dynamical system with clearances

N. Kranjcevic* University of Zagreb Zagreb, Croatia

M. Stegic† University of Zagreb Zagreb, Croatia

N. Vrankovic‡ University of Zagreb Zagreb, Croatia

Abstract— *Considering the time finite element method and the piecewise full decoupling method, the bifurcation in the harmonically excited two-degree-of-freedom dynamical system with clearances is investigated. The stability analysis based on the utilization of the Poincaré map is used in the time finite element procedure. In the piecewise full decoupling computations, the bifurcation analysis is performed by studying the periodicity of steady state solutions. Close agreement is found between the obtained results.*

Keywords: nonlinear vibrations, clearances, bifurcation

I. Introduction

Nonlinearities such as gaps and clearances exist in many dynamical systems either by design or due to manufacturing tolerances and wear. The characteristics of systems with clearances include abrupt variation of stiffness which is inherently nonlinear and difficulties that occur in their analysis exhibit great diversity.

In this paper, the bifurcation in the two-degree-of-freedom dynamical system with clearances, subjected to periodic excitations, is studied. The bifurcation analysis is performed considering the time finite element method and the piecewise full decoupling method. The system is assumed to be controlled by the excitation frequency (codimension-*one* bifurcation). A precise value of the excitation frequency, at which the bifurcation occurs is determined.

II. Problem formulation

The mechanical model of a two-degree-of-freedom system with clearances consists of two mass elements, two linear viscous dampers and two clearance type nonlinearities. The system is periodically excited. With $\boldsymbol{q}^{\mathrm{T}} = [q_1, q_2]$ being the nondimensional displacement, the equation of motion can be written as:

$$\boldsymbol{q}'' + \boldsymbol{Z}\,\boldsymbol{q}' + \boldsymbol{\Omega}\,\boldsymbol{h}(\boldsymbol{q}) = \boldsymbol{f}_0 + \boldsymbol{f}_{\mathrm{a}} \cos(\eta\tau) \tag{1}$$

where $\boldsymbol{h}^{\mathrm{T}}(\boldsymbol{q}) = \left[h(q_1), h(q_2)\right]$ is the nonlinear displacement vector, η denotes a nondimensional excitation frequency while $\boldsymbol{f}_0$ and $\boldsymbol{f}_{\mathrm{a}}$ are the amplitude vectors of mean and alternating load, respectively. Furthermore, the damping and stiffness matrices $\boldsymbol{Z}$ and $\boldsymbol{\Omega}$ are given as:

$$\boldsymbol{Z} = 2\begin{bmatrix} \zeta_{11} & -\zeta_{12}\omega_{12} \\ -\zeta_{21}\omega_{21} & \zeta_{22}\omega_{22} \end{bmatrix}, \quad \boldsymbol{\Omega} = \begin{bmatrix} 1 & -\omega_{12}^2 \\ -\omega_{21}^2 & \omega_{22}^2 \end{bmatrix}. \tag{2}$$

The nonlinear displacement vector is defined with the piecewise linear functions $h(q_i)$, i=1,2 that describe the clearance of value 2 (figure 1):

$$h(q_i) = \begin{cases} q_i + 1 & q_i < -1 \\ 0 & -1 \le q_i \le 1 \\ q_i - 1 & q_i > 1 \end{cases}. \tag{3}$$

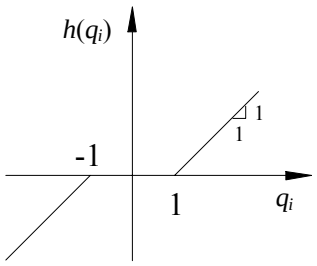

Fig. 1. Piecewise linear displacement function

Exact solutions of piecewise linear equations of motion are very rare and almost all of the solution methods are only approximate. A common solution method is the numerical time integration (Runge Kutta etc.), but this procedure can be very time consuming particular inside the frequency range of multi-valued responses and for lightly damped systems, since a great number of excitation periods must be simulated to obtain a steady state response.

A very efficient method for solving piecewise linear equations of motion in the frequency domain is the harmonic balance method [1], [2]. When the assumption of dominance of the first harmonic in the response is satisfied, the harmonic balance method is very accurate and numerically reliable procedure. If the influence of higher harmonic responses is significant, the method becomes very unreliable [13].

The incremental harmonic balance method [14] provides the study of effects of superharmonics and subharmonic to response and may be successfully applied to wide range of nonlinear diferential equations. This method is very

* E-mail: nenad.kranjcevic@fsb.hr
† E-mail: mstegic@fsb.hr
‡ E-mail: nvankov@fsb.hr

convenient for determining frequency response characteristics, because a new solution can be sought, with the previous solution used as very good approximation. A number of harmonics used in the solution is limited by numerical efficiency of the method, since the computer time grows geometrically with the number of harmonics in assumed solution.

The time finite element method [3], [12] is an implicit method for prediction of a steady state response of the nonlinear dynamical systems. Similar to the standard finite element technique, the time interval is divided into a finite number of time elements. The solution for all the spatial degrees of freedom at all time steps within a given time interval is sought through a set of algebraic equations.

The piecewise full decoupling method [4], [6] is a new developed numerical procedure of explicit integration based on coupling series of linear solutions, associated with piecewise linear functions. The accuracy of the method does not significantly depend on a magnitude of the integration step, since the results inside the linear part are based on analytical solutions.

A complete characterization of dynamical systems with clearances particularly requires determination of the stability of their steady state solutions. It is well known that under certain periodic excitations, the stiffness discontinuity in clearances can produce qualitative changes in the features of system, called bifurcations. The bifurcation is characterized by the fact that beyond the critical excitation frequency, the system moves away from its stable periodic behavior as soon as a small perturbation is superimposed.

III. Fundamentals of the time finite element method

The time finite element is based on Hamilton weak principle which describes the motion of the mechanical system between the two known nondimensional times τ_1 and τ_2:

$$\int_{\tau_1}^{\tau_2} (\delta L + \delta W)\,\mathrm{d}\tau = \delta \boldsymbol{q}^{\mathrm{T}}\ \boldsymbol{p}\Big|_{\tau_1}^{\tau_2} \tag{4}$$

where L and δW are the Lagrangian and the nonconservative virtual work, respectively, while $\boldsymbol{p}$ denotes the vector of the generalized momenta. Employing the equation (1), the Hamilton principle (4) can be written as:

$$\begin{aligned}&\int_{\tau_1}^{\tau_2} \left\{\delta \boldsymbol{q}'^{\mathrm{T}}\boldsymbol{q}' + \delta \boldsymbol{q}^{\mathrm{T}}[-\boldsymbol{Z}\boldsymbol{q}' - \boldsymbol{\Omega}\boldsymbol{h}(\boldsymbol{q}) + \boldsymbol{f}_0 + \boldsymbol{f}_{\mathrm{a}}\cos(\eta\tau)]\right\}\mathrm{d}\tau \\ &= \delta \boldsymbol{q}^{\mathrm{T}}\ \boldsymbol{p}\Big|_{\tau_1}^{\tau_2}\end{aligned} \tag{5}$$

The basis of the time finite element procedure is, the division of the time interval $\tau_2 - \tau_1$ (equals to the period of excitation) into a finite number n_e of time elements and the approximation of the displacement $\boldsymbol{q}_j(\tau)$ within each time element using the standard finite element interpolation:

$$\begin{aligned}&\boldsymbol{q}_j(\tau) = \boldsymbol{N}_j(\tau)\,\overline{\boldsymbol{q}}_j, \\ &\boldsymbol{q}'_j(\tau) = \boldsymbol{N}'_j(\tau)\,\overline{\boldsymbol{q}}_j,\ \ j=1(1)n_{\mathrm{e}}\end{aligned} \tag{6}$$

where $\boldsymbol{N}_j$ is the shape function and $\overline{\boldsymbol{q}}_j$ denotes the nodal displacement. The above interpolation inserted into the integral form (5) at time element level results in the local finite element equation:

$$\boldsymbol{A}_j\,\overline{\boldsymbol{q}}_j + \boldsymbol{g}_j(\overline{\boldsymbol{q}}_j) + \boldsymbol{f}_j = \boldsymbol{p}_j,\quad j=1(1)n_{\mathrm{e}} \tag{7}$$

where:

$$\begin{aligned}&\boldsymbol{A}_j = \int_{\tau_j}^{\tau_{j+1}} [\boldsymbol{N}_j'^{\mathrm{T}}\boldsymbol{N}'_j - \boldsymbol{N}_j^{\mathrm{T}}\boldsymbol{Z}\boldsymbol{N}'_j]\,\mathrm{d}\tau, \\ &\boldsymbol{g}_j(\overline{\boldsymbol{q}}_j) = -\int_{\tau_j}^{\tau_{j+1}} \boldsymbol{N}_j^{\mathrm{T}}\boldsymbol{\Omega}\boldsymbol{h}(\boldsymbol{q})\,\mathrm{d}\tau, \\ &\boldsymbol{f}_j = \int_{\tau_j}^{\tau_{j+1}} [\boldsymbol{N}_j^{\mathrm{T}}\boldsymbol{f}_0 + \boldsymbol{N}_j^{\mathrm{T}}\boldsymbol{f}_{\mathrm{a}}\cos(\eta\tau)]\,\mathrm{d}\tau.\end{aligned} \tag{8}$$

The global element equation can be determined by assembling the finite element equations at the time element level (7), as in the standard finite element modeling scheme, yielding:

$$\boldsymbol{A}\overline{\boldsymbol{q}} + \boldsymbol{g}(\overline{\boldsymbol{q}}) + \boldsymbol{f} = \boldsymbol{0} \tag{9}$$

where, with a summation notation representing the element assemblage operation:

$$\begin{aligned}&\overline{\boldsymbol{q}} = \sum_{j=1}^{n_e} \overline{\boldsymbol{q}}_j,\quad \boldsymbol{A} = \sum_{j=1}^{n_e} \boldsymbol{A}_j, \\ &\boldsymbol{g}(\overline{\boldsymbol{q}}) = \sum_{j=1}^{n_e} \boldsymbol{g}_j(\overline{\boldsymbol{q}}_j),\quad \boldsymbol{f} = \sum_{j=1}^{n_e} \boldsymbol{f}_j\end{aligned}. \tag{10}$$

For a periodic solution, the term on the right-side of the equation (9) vanishes, as the periodic boundary condition requires both displacements and generalized momenta to be identical at τ_1 and τ_2. The global finite element equation is a set of nonlinear algebraic equations in unknown nodal displacement vector $\overline{\boldsymbol{q}}$ which can be determined employing one of iteration methods. Considering Newton-Raphson method, the nodal displacement $\overline{\boldsymbol{q}}$ is iterated as:

$$\overline{\boldsymbol{q}}^{(n+1)} = \overline{\boldsymbol{q}}^{(n)} + \Delta\overline{\boldsymbol{q}}^{(n)} \tag{11}$$

For a small increment $\Delta\overline{\boldsymbol{q}}^{(n)}$, the equation (9), can be expanded into Taylor series retaining only the linear

terms:

$$\boldsymbol{d}^{(n)} + \boldsymbol{K}^{(n)} \Delta\overline{\boldsymbol{q}}^{(n)} = \boldsymbol{0} \tag{12}$$

where:

$$\boldsymbol{d}^{(n)} = \boldsymbol{A}\,\overline{\boldsymbol{q}}^{(n)} + \boldsymbol{g}^{(n)}(\overline{\boldsymbol{q}}) + \boldsymbol{f}, \quad \boldsymbol{K}^{(n)} = \boldsymbol{A} + \frac{\partial \boldsymbol{g}^{(n)}(\overline{\boldsymbol{q}})}{\partial \overline{\boldsymbol{q}}^{(n)}}. \tag{13}$$

Since the components of the stiffness vector $\boldsymbol{g}^{(n)}$, depend on the piecewise linear displacement function (3), the iteration procedure needs their computations at each iteration step. The components of matrix $\boldsymbol{A}$ and vector $\boldsymbol{f}$ are constants and they need to be calculated only once. The iteration procedure defined by the equations (11), (12) will be terminated when the increment $\Delta\overline{\boldsymbol{q}}^{(n)}$ converges towards zero.

The stability of time finite element solutions can be examined as the stability of the Poincaré map. Let:

$$\boldsymbol{s}^{\mathrm{T}} = \left[\Delta\overline{\boldsymbol{q}}, \boldsymbol{p}\right] \tag{14}$$

be a point on the Poincaré section (fixed point). For convenience and without loss of generality, in the equations (14), the velocity is substituted with the generalized momenta $\boldsymbol{p}$. For the periodic solution, the Poincaré map $\boldsymbol{P}$ is defined as:

$$\boldsymbol{P}(\boldsymbol{s}) = \boldsymbol{x}(\boldsymbol{s}, \tau_1, \tau_2) = \boldsymbol{s} \tag{15}$$

i.e. the periodic orbit $\boldsymbol{x}(\boldsymbol{s}, \tau_1, \tau_2)$ obviously corresponds to a fixed point on the Poincaré section. In a neighborhood of the fixed point, we have:

$$\boldsymbol{P}(\boldsymbol{s} + \boldsymbol{v}) = \boldsymbol{P}(\boldsymbol{s}) + \frac{\partial \boldsymbol{P}}{\partial \boldsymbol{s}}\boldsymbol{v} + \boldsymbol{O}(\left\|\boldsymbol{v}^2\right\|) \tag{16}$$

where $\left\|\boldsymbol{v}\right\|$ is the norm of the deviation from the fixed point. Information on the stability of the fixed point can be obtained by studying the eigenvalues of the Jacobian matrix $\partial\boldsymbol{P}/\partial\boldsymbol{s}$. If the eigenvalues are inside the unit circle the system is asymptotically stable; if at least one of the eigenvalues is outside the circle the system is unstable. The stability boundary is the unit circle itself. There are two possible scenarios in which the eigenvalues may leave the unit circle. First, real eigenvalues of the Jacobian matrix leave the unit circle through ± 1, resulting in a generalized static bifurcation (transcritical, symmetry-breaking, cyclic-fold or period-doubling). Second, complex conjugate eigenvalues leave the unit circle away from the real axis, resulting in a generalized Hopf (Neimark) bifurcation.

To incorporate determination of the eigenvalues of Poincaré map in the time finite element procedure, we have to return to the incremental finite element equation (12) at the time element level:

$$\boldsymbol{d}_j + \boldsymbol{K}_j\,\Delta\overline{\boldsymbol{q}}_j = \boldsymbol{p}_j. \tag{17}$$

The above equation can be partitioned as:

$$\begin{bmatrix}\boldsymbol{d}_{\mathrm{B}}\\ \boldsymbol{d}_{\mathrm{I}}\end{bmatrix}_j + \begin{bmatrix}\boldsymbol{K}_{\mathrm{BB}} & \boldsymbol{K}_{\mathrm{BI}}\\ \boldsymbol{K}_{\mathrm{IB}} & \boldsymbol{K}_{\mathrm{II}}\end{bmatrix}_j \begin{bmatrix}\Delta\overline{\boldsymbol{q}}_{\mathrm{B}}\\ \Delta\overline{\boldsymbol{q}}_{\mathrm{I}}\end{bmatrix}_j = \begin{bmatrix}\boldsymbol{p}_{\mathrm{B}}\\ \boldsymbol{0}\end{bmatrix}_j \tag{18}$$

where B and I correspond to the temporal nodes at the ends and in the interior of time element j, respectively, while $\boldsymbol{p}_{\mathrm{B}_j}^{\mathrm{T}} = \left[-\boldsymbol{p}(\tau_j),\ \ \boldsymbol{p}(\tau_{j+1})\right]$ denotes the vector of momenta at the boundary nodes. Compare the lower part with the upper part of the equation (18) to eliminate the interior nodal displacement $\Delta\overline{\boldsymbol{q}}_{\mathrm{I}\,j}$:

$$\begin{aligned}&(\boldsymbol{d}_{\mathrm{B}} - \boldsymbol{K}_{\mathrm{BI}}\,\boldsymbol{K}_{\mathrm{II}}^{-1}\,\boldsymbol{d}_{\mathrm{I}})_j +\\ &(\boldsymbol{K}_{\mathrm{BB}} - \boldsymbol{K}_{\mathrm{BI}}\,\boldsymbol{K}_{\mathrm{II}}^{-1}\,\boldsymbol{K}_{\mathrm{IB}})_j \Delta\overline{\boldsymbol{q}}_{\mathrm{B}j} = \boldsymbol{p}_{\mathrm{B}j}\end{aligned}. \tag{19}$$

Considering the assemblage procedure, the equation (19) of all time elements are further condensed by imposing the compatibility conditions at the common node of the two elements, yielding the elimination of the common node. This procedure results into the global equation:

$$\begin{bmatrix}\boldsymbol{d}_1\\ \boldsymbol{d}_2\end{bmatrix} + \begin{bmatrix}\boldsymbol{K}_{11} & \boldsymbol{K}_{12}\\ \boldsymbol{K}_{21} & \boldsymbol{K}_{22}\end{bmatrix}\begin{bmatrix}\Delta\overline{\boldsymbol{q}}_1\\ \Delta\overline{\boldsymbol{q}}_2\end{bmatrix} = \begin{bmatrix}-\boldsymbol{p}_1\\ \boldsymbol{p}_2\end{bmatrix} \tag{20}$$

where 1 and 2 denote the initial and final time nodes. The equation (20) can be reformulated as the relationship between the fixed points at the ends of period $\boldsymbol{s}_2$ and $\boldsymbol{s}_1$ which leads to the Jacobian matrix:

$$\partial\boldsymbol{P}/\partial\boldsymbol{s} = \begin{bmatrix}-\boldsymbol{K}_{12}^{-1}\boldsymbol{K}_{11} & -\boldsymbol{K}_{12}^{-1}\\ \boldsymbol{K}_{21} - \boldsymbol{K}_{22}\boldsymbol{K}_{12}^{-1}\boldsymbol{K}_{11} & -\boldsymbol{K}_{22}\boldsymbol{K}_{12}^{-1}\end{bmatrix}. \tag{21}$$

IV. Piecewise full decoupling method

The piecewise full decoupling method is based on the substitution of the piecewise linear equation of motion (1) with a set of linear equations of motion, defined inside each of the stage stiffness region:

$$\boldsymbol{q}'' + \boldsymbol{Z}\boldsymbol{q}' + \boldsymbol{\Pi}_{k\Omega}\boldsymbol{q} = \boldsymbol{b}_{k\Omega} + \boldsymbol{f}_0 + \boldsymbol{f}_{\mathrm{a}}\cos(\eta\tau),\ k = 1(1)9 \tag{22}$$

where:

$$\begin{aligned}&\boldsymbol{\Pi}_{1\boldsymbol{\Omega}} = \boldsymbol{\Pi}_{3\boldsymbol{\Omega}} = \boldsymbol{\Pi}_{7\boldsymbol{\Omega}} = \boldsymbol{\Pi}_{9\boldsymbol{\Omega}} = \boldsymbol{\Omega},\\ &\boldsymbol{\Pi}_{2\boldsymbol{\Omega}} = \boldsymbol{\Pi}_{8\boldsymbol{\Omega}} = \begin{bmatrix}1 & 0\\ -\omega_{21}^2 & 0\end{bmatrix},\\ &\boldsymbol{\Pi}_{4\boldsymbol{\Omega}} = \boldsymbol{\Pi}_{6\boldsymbol{\Omega}} = \begin{bmatrix}1 & -\omega_{12}^2\\ 0 & \omega_{22}^2\end{bmatrix}, \quad \boldsymbol{\Pi}_{5\boldsymbol{\Omega}} = \boldsymbol{0}\end{aligned} \tag{23}$$

denote the local stiffness matrices while:

$$\boldsymbol{b}_{1\Omega}^{\mathrm{T}} = -\boldsymbol{b}_{9\Omega}^{\mathrm{T}} = \left[(1 - \omega_{12}^2),\ \ (-\omega_{21}^2 + \omega_{22}^2)\right],$$

$$\boldsymbol{b}_{2\Omega}^{\mathrm{T}} = -\boldsymbol{b}_{8\Omega}^{\mathrm{T}} = \left[1, -\omega_{21}^2\right],$$

$$\begin{aligned} \boldsymbol{b}_{3\Omega}^{\mathrm{T}} &= -\boldsymbol{b}_{7\Omega}^{\mathrm{T}} = \left[(1+\omega_{12}^2),\quad -(\omega_{21}^2+\omega_{22}^2)\right], \\ \boldsymbol{b}_{4\Omega}^{\mathrm{T}} &= -\boldsymbol{b}_{6\Omega}^{\mathrm{T}} = \left[-\omega_{12}^2, -\omega_{22}^2\right], \quad \boldsymbol{b}_{5\Omega}^{\mathrm{T}} = [0,\,0] \end{aligned} \tag{24}$$

are the vectors of the breakpoints. The dynamical system with clearances starts from an initial position described with one of the local equation of motion. When the system changes a stage stiffness region, the system is represented with new local equation of motion. The determination of times in which the system changes a stiffness region can be done only numerically.

Each of the local equations of motion (22) has been solved by applying the state-space formulation. The state vector $\boldsymbol{y} = \left[\boldsymbol{q},\ \boldsymbol{q}'\right]^{\mathrm{T}}$ implies the state matrix $\boldsymbol{A}$ of the form:

$$\boldsymbol{A} = \begin{bmatrix} \boldsymbol{0} & \boldsymbol{I} \\ -\boldsymbol{\Pi}_{k\Omega} & -\boldsymbol{Z} \end{bmatrix}. \tag{25}$$

The matrix $\boldsymbol{A}$ is a real nonsymmetric matrix and its eigenvalues can be calculated using one of numerical routines for the nonsymmetric eigenvalue problem. Obtained eigenvalues enable the similarity transformation which uncouples the equations of motion giving:

$$\boldsymbol{z}' = \boldsymbol{\Lambda}\boldsymbol{z} + \boldsymbol{h} \tag{26}$$

where $\boldsymbol{z}$ denotes the normal coordinate, $\boldsymbol{\Lambda} = \mathrm{diag}(\lambda_l),\ l = 1(1)4$ is the matrix of eigenvalues and $\boldsymbol{h}$ is the excitation vector. The equation (26) has well-known analytical solutions.

The piecewise full decoupling method is an explicit integration method and the stability of solutions cannot be studied considering the standard stability procedures such as Poincaré map or Floquet theory. The responses obtained by explicit metods can be only classified as either periodic or nonperiodic. Nonperiodic responses may corespond to a quasiperiodic, transient or chaotic motion. Therefore, the stability of solutions has to be investigated by studying the periodicity of responses. If the steady state amplitude:

$$\bar{q} = \frac{q_{\max} - q_{\min}}{2} \tag{27}$$

coincides with the effective amplitude:

$$q_{\mathrm{ef}} = \sqrt{\frac{2}{T}\int_0^T (q(t) - q_{\mathrm{av}})^2\,\mathrm{d}t} \tag{28}$$

the response is periodic; otherwise the response is nonperiodic. In the equation (28), T denotes the period of motion while q_{av} is the average of the $q(t)$:

$$q_{\mathrm{av}} = \frac{1}{T}\int_0^T q(t)\,\mathrm{d}t\ . \tag{29}$$

V. Results

The piecewise full decoupling method and the time finite element method are applied to determine the bifurcation point of the two-degree-of-freedom dynamical system with two clearances. The system parameters $\zeta_{11} = \zeta_{12} = \zeta_{21} = \zeta_{22} = 0.05$, $\omega_{12} = \omega_{21} = 0.6$, $\omega_{22} = 1.1$, $\boldsymbol{f}_0^{\mathrm{T}} = \left[0.5,\ 0.25\right]$ and $\boldsymbol{f}_{\mathrm{a}}^{\mathrm{T}} = \left[0.25,\ 0\right]$ are adopted from [9] where the system with one clearance was studied using the harmonic balance method.

Starting from the trivial initial condition, the piecewise full decoupling computations are performed simulating 128 excitation periods for the single point of excitation frequency. This procedure is well suited [11] because no another reliable way to distinguish the transient and steady state motion at chaotic responses. The switch points in each stage stiffness region and the eigenvalues of the state matrix were computed employing the MATLAB routines FZERO and EIG. The frequency response in figure 2 indicates the frequency range of the uncorresponding solutions for steady state and effective amplitudes. The separation of the amplitudes (bifurcation point) starts at $\eta = 0.767$ as shown in figure 3.

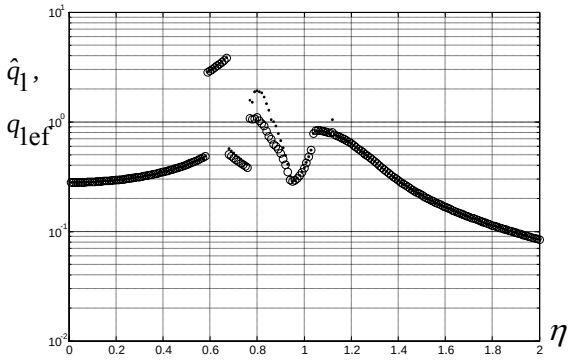

Fig. 2. Frequency response obtained by the piecewise full decoupling method; • steady state amplitude $\hat{q}_1$, ◦ effective amplitude $q_{1\mathrm{ef}}$

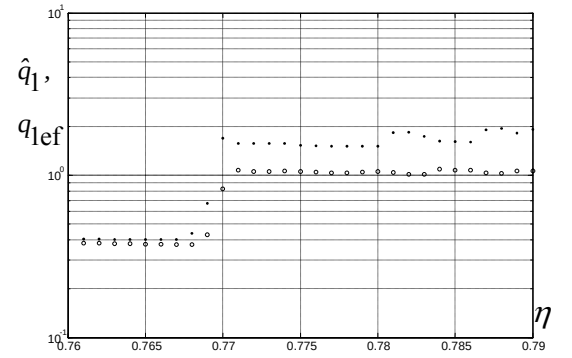

Fig. 3. Separation of the steady state and effective amplitudes; • steady state amplitude $\hat{q}_1$, ◦ effective amplitude $q_{1\mathrm{ef}}$

These results are verified with the time finite element method. The finite element calculations were performed

with ten four nodes time elements (the third order polynomials are taken as shape functions). The iteration procedure limited on 100 iterations was accompanied with the stability analysis by the Poincaré map. Considering the response of the linear system as the starting vector, the unconverged or unstable solutions are found in the frequency range $0.7 < \eta < 0.96$ (figure 4). Using the previous stable solution as the starting vector only unstable solutions are found, but within narrow bounds $0.77 < \eta < 0.94$ (figure 5).

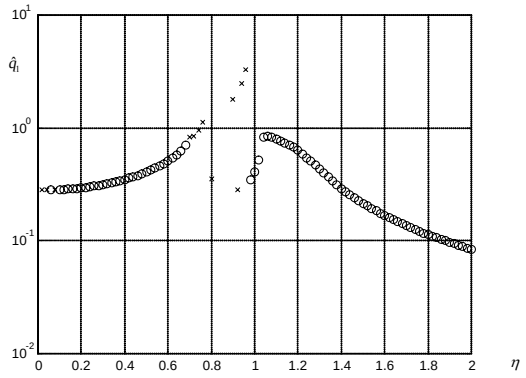

Fig. 4. Frequency response obtained by the time finite element method (starting vector-response of linear system); ○ stable solution, x unstable solution or achieved maximum of 100 iterations

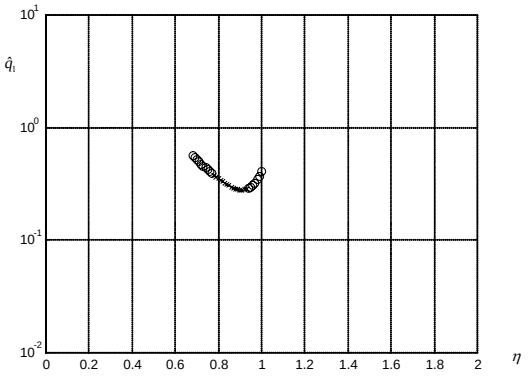

Fig. 5. Frequency response obtained with the previous stable solution as the starting vector; ○ stable solution, x unstable solution

Imposing small increments in the excitation frequency, the bifurcation point can be precisely determined. For the excitation frequency $\eta = 0.772$, the eigenvalues of the Poincarè map are:

$$\begin{aligned} \lambda_{1,2} &= -0.0527 \pm 0.9939i, \quad |\lambda_{1,2}| = 0.9953 \\ \lambda_{3,4} &= 0.0266 \pm 0.4267i, \quad |\lambda_{3,4}| = 0.4275 \end{aligned} \tag{30}$$

(asymptotically stable solution), while for the excitation frequency $\eta = 0.773$ the eigenvalues yield:

$$\begin{aligned} \lambda_{1,2} &= -0.0496 \pm 0.9996i, \quad |\lambda_{1,2}| = 1.0008 \\ \lambda_{3,4} &= 0.0280 \pm 0.4247i, \quad |\lambda_{3,4}| = 0.4256 \end{aligned} \tag{31}$$

(unstable solution). These results indicate that a complex conjugate pair of the eigenvalues crosses the unit circle away from the real axis resulting in Neimark bifurcation.

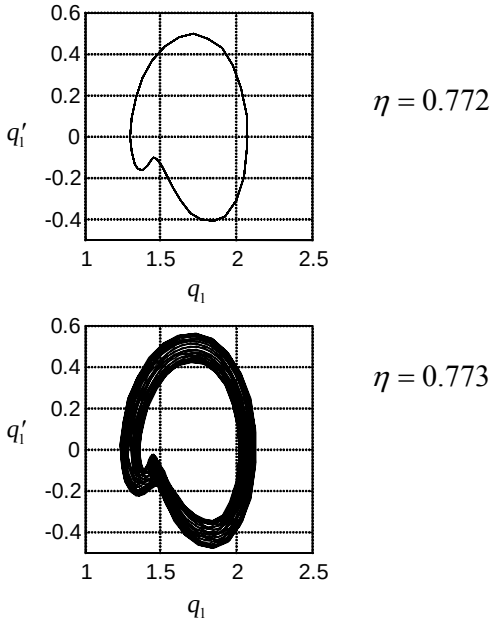

Fig. 6. Phase portraits showing the Neimark bifurcation

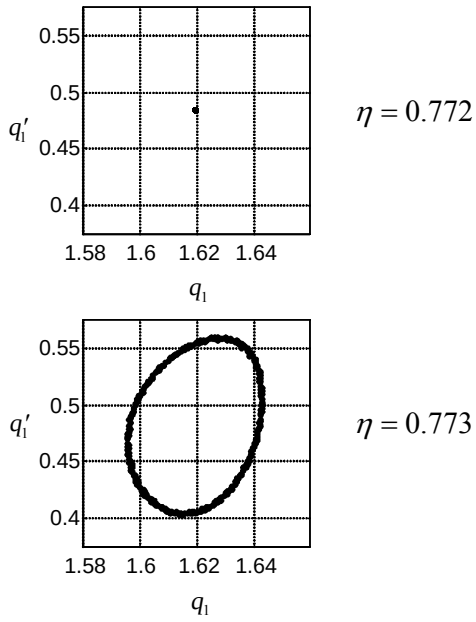

Fig. 7. Poincarè sections showing the Neimark bifurcation

The phase portraits and Poincarè sections of the bifurcating solution are determined by using the piecewise full decoupling method. Simulation procedure was performed with 4096 excitation periods in transient part regarding the displacements and velocities at the first node of the time finite element mesh as the initial conditions. The patterns in figures 6, 7 confirm the Neimark bifurcation.

The bifurcation point obtained by the piecewise full decoupling method and the time finite element method is not in agreement. This disagreement can be understood knowing that the time finite element method cannot solve problems with ideal clearance because the zero stiffness implies the singularity of the tangent matrix $\boldsymbol{K}^{(n)}$. In the finite element calculations, the clearance nonlinearity (3) was approximated by the trilinear system at which the slope of the second stage is 1% of the slope of the first and third stages.

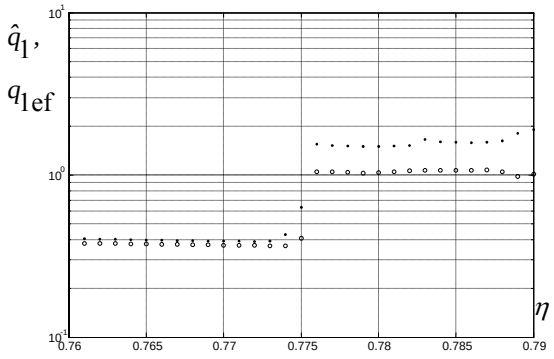

Fig. 8. Frequency response obtained by the piecewise full decoupling method (clearances are modelled as trilinear system);
• steady state amplitude $\hat{q}_1$, ◦ effective amplitude q_{1ef}

Modelling the clearances with the above described trilinear system, repeated piecewise full decoupling computations (figure 8) agree very well with the results of the time finite element method (30) and (31).

VI. Conclusions

The local bifurcation in a dynamical system with clearances is a qualitative change of its behaviour which occurs as the consequence of stiffness discontinuity. In this paper, the bifurcation of the two-degree-of-freedom dynamical system with clearances is studied by using the time finite element method and the piecewise full decoupling method. Comparison of the proposed bifurcation analyses shows that both procedures give very accurate results.

References

[1] Chatterjee S., Mallik A.K. and Ghosh A. Periodic response of piecewise non-linear oscillators under harmonic excitation. *Journal of Sound and Vibration*, 191(1): 129-144, March 1996.

[2] Kahraman A. and Singh R. Nonlinear dynamics of a spur gear pair. *Journal of Sound and Vibration*, 142(1): 49-75, October 1990.

[3] Kranjcevic N., Stegic M. and Vrankovic N. Nonlinear problems in dynamics by the finite element in time method. *In Int. Conf. on Applied Mathematics and Scientific Computing*, pages 211-219, Dubrovnik, June 4-8, 2001.

[4] Kranjcevic N., Stegic M. and Vrankovic N. The piecewise full decoupling method for dynamic problems. *Proceedings in Applied Mathematics and Mechanics,* 3(1): 112-113, December 2003.

[5] Kranjcevic N., Stegic M. and Vrankovic N. Stability and bifurcation analysis of a two-degree-of-freedom system with clearances. *In 3rd MIT Conf. on Computational Fluid and Solid Mechanics,* pages 297-301, Cambridge, June 14-17, 2005.

[6] Kranjcevic N., Stegic M. and Vrankovic N. Method for computing steady state response of dynamical systems with clearances. *In 8th Int. Conf. on Computational Plasticity*, pages 1146-1149, Barcelona, September 5-7, 2005.

[7] Meirovitch L. *Principles and techniques of vibratons*. Prentice-Hall, 1997.

[8] Nayfeh A.H. and Balachandran B. *Applied nonlinear dynamics*. John Wiley, 1995.

[9] Padmanabhan C. and Singh R. Spectral coupling issues in a two-degree-of-freedom system with clearance non-linearities. *Journal of Sound and Vibration*, 155(2): 209-230, June 1992.

[10] Stegic M., Vrankovic N. and Kranjcevic N. Frequency response of a mechanical system with multiple clearances using the piecewise full decoupling method and the time finite element method. *In 11th World Congress in Mechanism and Machine Science*, pages 552-556, Tianjin, April 1-4, 2004.

[11] Thompson J.M.T. and Stewart H.B. *Nonlinear dynamics and chaos: Geometrical methods for engineers and scientists*. John Wiley, 1986.

[12] Wang Y. Dynamics of unsymmetric piecewise-linear/non-linear systems using finite elements in time. *Journal of Sound and Vibration*, 185(1): 155-170, August 1995.

[13] Wolf H.. and Stegić M. The influence of neglecting small harmonic terms on estimation of dynamical stability of the response of non-linear oscillators. *Computational Mechanics*, 24(4): 230-237, October 1999.

[14] Wong C.W. Zhang W.S. and Lau S.L. Periodic forced vibration of unsymmetrical piecewise-linear systems by incremental harmonic balance method. *Journal of Sound and Vibration*, 149(1): 91-105, August 1991.